Electronic Supplementary Information

for

Cu(II)-Specific Metallogel Formation by an Amido-Anthraquinone-Pyridyloxalamide Ligand in DMSO-water.

Massimo Cametti,* Mario Cetina and Zoran Džolić*

[a] Department of Chemistry, Materials and Chemical Engineering "Giulio Natta", Politecnico di Milano, Via L. Mancinelli 7, 20131 Milano, Italy; E-mail: massimo.cametti@polimi.it
[b] University of Zagreb, Faculty of Textile Technology, Department of Applied Chemistry, Prilaz baruna Filipovića 28a, 10000 Zagreb, Croatia
[c] Rudjer Bošković Institute, Bijenička cesta 54, 10000 Zagreb, Croatia; E-mail: zoran.dzolic@irb.hr

Table of content:

Materials and Methods.

Reagents were purchased from Aldrich or Fluka and were used without further purification. All solvents were purified and dried according to standard procedures. Thin-layer chromatography (t.l.c.) was performed on Merck Kieselgel HF254 plastic sheets and spots were made visible using a UV lamp (254 nm) or I_2 vapours.All solvents were purified and dried by standard procedures and distilled prior to use. Melting points were determined on a Kofler hot-stage apparatus and are uncorrected. ^{1}H and ^{13}C NMR spectra were recorded with a Bruker AV 300 and 400 spectrometer. Chemical shifts, in ppm, are referred to TMS as internal standard or to residual solvent peak. The FT-IR spectra were recorded at a resolution of 4 cm^{-1} on an ABB Bomem MB102 single beam FT-IR spectrometer.

General procedure for the synthesis of ligands 4-6:

Picolylamine (6.0 mmol) and a catalytic amount of 4-dimethylaminopyridine (DMAP) were added to a solution of ethyl *N*-(1-aminoanthraquinone)oxalamate[S1] (5.42 mmol) in dry CH_2Cl_2 (30 mL). After the mixture was stirred at room temperature for 2 days, the reaction mixture was filtered off and recrystallized from DMF to afford the product as yellow solid.

***N*-(1-aminoanthraquinone)-*N'*-(pyridin-2-ylmethyl)oxalamide (4)**

Yield 86 %; mp 257 °C; ^{1}H NMR (DMSO-d_6): δ = 13.45 (s, 1H, -*NH*CO), 9.34 (br t, 1H, CH_2*NH*), 9.06 (dd, *J* = 8.3 and 1.3, 1H, Ar-CH), 8.55 (d, *J* = 4.7, 1H, C-H$_{Pic}$), 8.22 (m, 2H, Ar-CH), 7.98 (m, 4H, Ar-CH), 7.78 (m, 1H, C-H$_{Pic}$), 7.40 (d, *J* = 7.9, 1H, C-H$_{Pic}$), 7.29 (m, 1H, C-H$_{Pic}$), 4.61 (d, *J* = 6.0, 2H, *CH$_2$*NH); ^{13}C NMR (DMSO-d_6): δ = 45.1, 119.6, 121.8, 122.8, 123.3, 125.7, 126.9, 127.6, 132.8, 134.2, 134.6, 135.2, 135.3, 136.2, 137.4, 139.9, 149.2, 157.5, 159.7, 160.2, 182.6, 186.7; IR (KBr): ν = 3364, 3188, 1700, 1667, 1647, 1582, 1512, 1419, 1340; Elemental analysis calcd (%) for $C_{22}H_{15}N_3O_4$: C 68.57 H 3.92 N 10.90; found C 68.50 H 3.95 N 10.89.

***N*-(1-aminoanthraquinone)-*N'*-(pyridin-3-ylmethyl)oxalamide (5)**

Yield 90 %; mp 289 °C; ^{1}H NMR (DMSO-d_6): δ = 13.45 (s, 1H, -*NH*CO), 9.78 (t, *J* = 6.0, 1H, CH_2*NH*), 9.05 (dd, *J* = 8.2 and 1.4, 1H, Ar-CH), 8.58 (d, *J* = 1.7, 1H, C-H$_{Pic}$), 8.48 (dd, *J* = 4.8 and 1.6, 1H, C-H$_{Pic}$), 8.22 (m, 2H, Ar-CH), 7.98 (m, 4H, Ar-CH), 7.77 (m, 1H, C-H$_{Pic}$), 7.38 (m, 1H, C-H$_{Pic}$), 4.47 (d, *J* = 6.3, 2H, *CH$_2$*NH); ^{13}C NMR (DMSO-d_6): δ = 40.6, 119.0, 122.7, 123.4, 123.5, 125.1, 126.4, 127.0, 132.2, 133.9, 134.0, 134.6, 134.7, 135.3, 135.6, 139.3, 148.3, 148.9, 159.0, 159.6, 182.1, 186.1; IR (KBr): ν = 3171, 1708, 1670, 1652, 1583, 1507, 1421, 1338; Elemental analysis calcd (%) for $C_{22}H_{15}N_3O_4$: C 68.57 H 3.92 N 10.90; found C 68.46 H 3.90 N 10.91.

***N*-(1-aminoanthraquinone)-*N'*-(pyridin-4-ylmethyl)oxalamide (6)**

Yield 92 %; mp 272 °C; ^{1}H NMR (DMSO-d_6): δ = 13.45 (s, 1H, -*NH*CO), 9.80 (t, *J* = 6.3, 1H, CH_2*NH*), 9.07 (dd, *J* = 8.1 and 1.3, 1H, Ar-CH), 8.68 (d, *J* = 6.0, 2H, C-H$_{Pic}$), 8.22 (m, 2H, Ar-CH), 7.99 (m, 4H, Ar-CH), 7.34 (d, *J* = 5.9, 2H, C-H$_{Pic}$), 4.47 (d, *J* = 6.3, 2H, *CH$_2$*NH); ^{13}C NMR (DMSO-d_6 + TFA): δ = 42.8, 119.2, 123.1, 125.3, 125.5, 126.7, 127.2, 132.5, 133.9, 134.3, 134.9, 135.9, 139.6, 141.8, 158.0, 158.4, 158.8, 158.9, 159.4, 160.5, 182.3, 186.5 ; IR (KBr): ν = 3349,

3103, 1700, 1677, 1650, 1589, 1509, 1420, 1332; Elemental analysis calcd (%) for $C_{22}H_{15}N_3O_4$: C 68.57 H 3.92 N 10.90; found C 68.60 H 3.95 N 10.91.

Gelation experiments:

A weighed amount of the ligand (10 mg) and metal salt were combined in different stoichiometric ratio in various solvents (1.0 mL total) into a sealed glass vial and heated. The mixture was then cooled to room temperature and checked for the possible gel formation. Gelation behaviour was tested with the following solvents or solvent mixtures: water, DMSO, DMSO–water, DMF, DMF–water, MeOH, EtOH, dioxane, THF, EtOAc, acetone, CH_2Cl_2, CH_3CN, toluene, *p*-xylene and benzene. No sign of gelation was observed but with **4** in DMSO or DMSO-water mixture

Metallo-gel formation in DMSO/H_2O (v/v = 9:1) was obtained by adding the ligand, $CuCl_2{\cdot}2H_2O$ and the solvents in a screw-capped sample tube and then heating till a transparent solution was obtained. After cooling to room temperature, the gel was formed and confirmed by confirmed by "test tube inversion" method.

Figure S1. Photographs of sol–gel transition between the dark yellow solution and the green metallogel of **4**/$CuCl_2$ (0.05 M,1:1 ratio) in 90% DMSO/water solvent mixture.

Table S1. Minimum number of equivalents of Cu(II) salt added to **4** for gelation and T_{gel}

Concentration of ligand **4** (M)	**No. of $CuCl_2$ equivalents (T_{gel} / °C)**	**No. of $CuBr_2$ equivalents (T_{gel} / °C)**
0.100	1 (102)	1 (91)
0.050	1 (96)	2 (84)
0.035	2 (88)	3 (77)
0.025	3 (84)	5 (72)
0.020	7 (82)	9 (67)
0.010	14 (75)	25 (63)
0.005	no gels >55 (-)	-

Thermal Stability:

The thermal stability of the gels was determined using the dropping ball method whereby 3 mL of gel were prepared as described above in a sample vial (diameter 20 mm). A steel ball (diameter 5 mm, mass 1.40 g) was carefully placed in the middle of the surface of the gel and the vial was then sealed and immersed in an oil bath. Upon heating the gel-sol transition temperature (T_{gel}) was recorded when the ball had completely sunk into the gel.

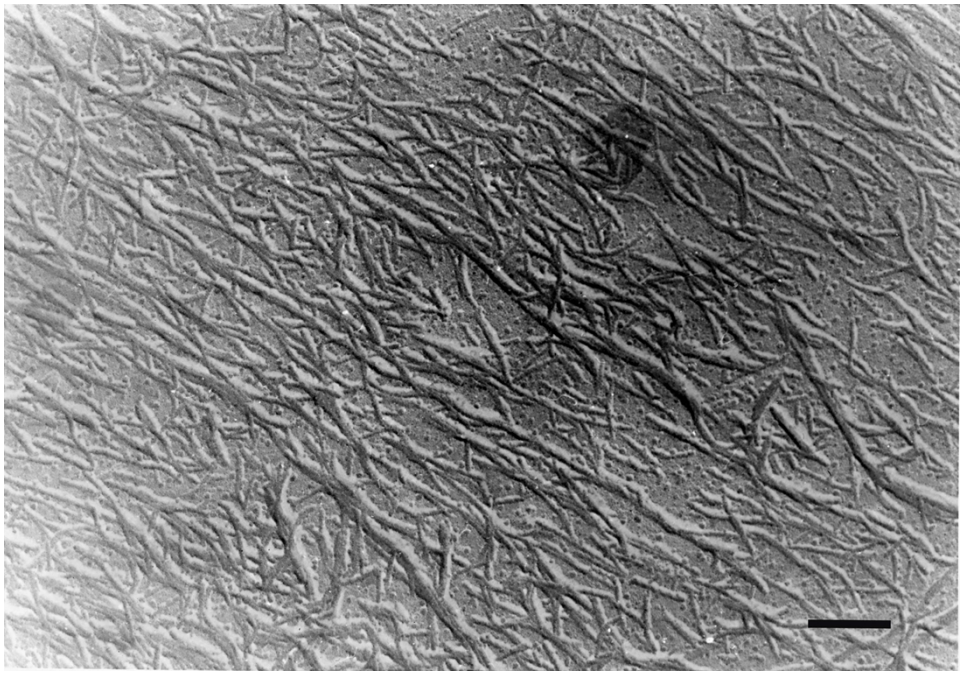

Figure S2. TEM image of the **4**/$CuCl_2$ metallogel in 90% DMSO (1:1 M/L ratio, 0.05 M) reveal the presence of a dense nanofiber network (scale bar = 250 nm).

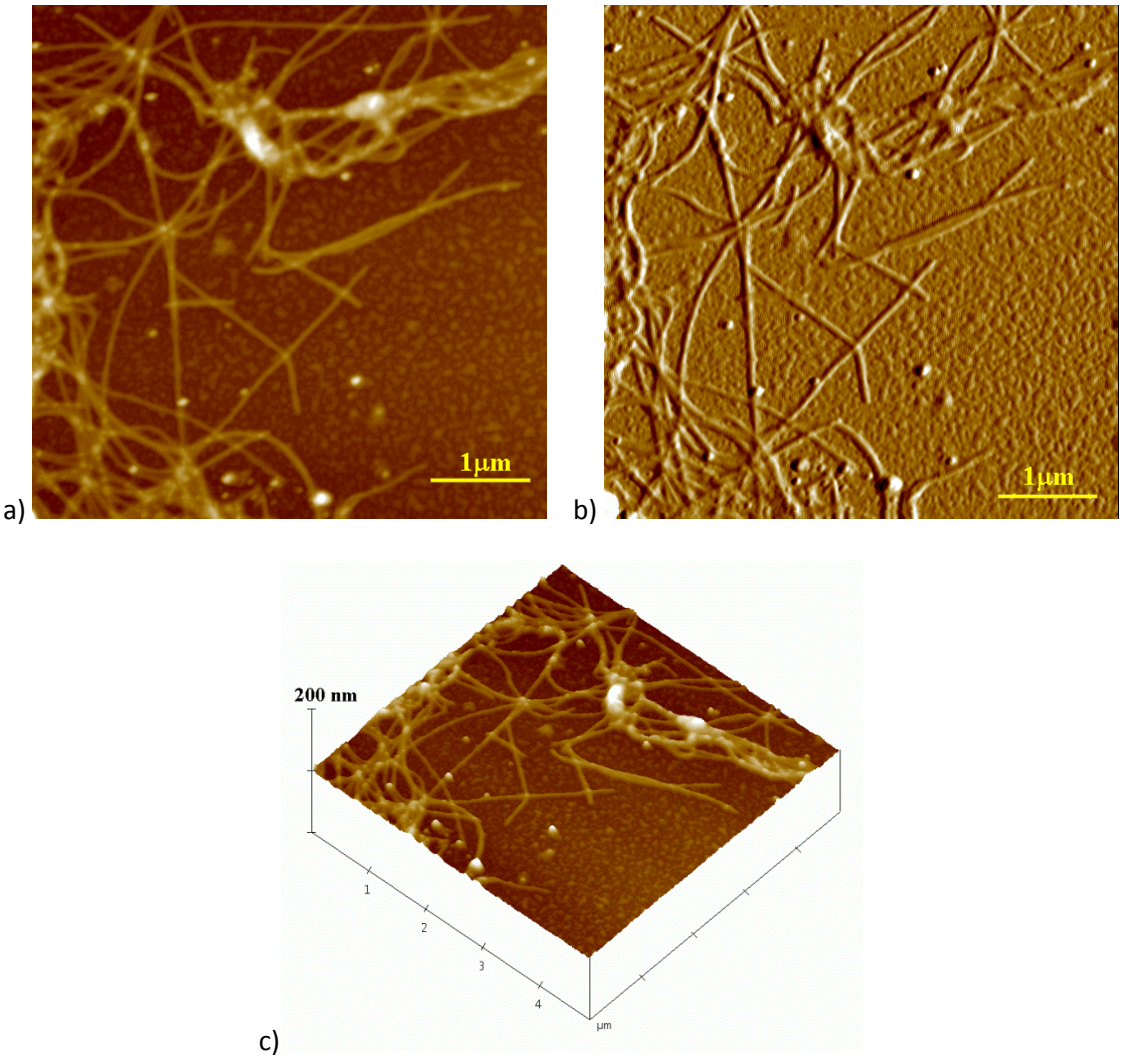

Figure S3. An example of the AFM images of the **4**-$CuCl_2$ gel system (1:1, [**4**] = 0.05 M) in 10% DMSO captured in air at 24.5 °C: a) 2D height image with vertical scale 60 nm; b) the corresponding amplitude image and c) 3D height image 5×5 μm scan area.

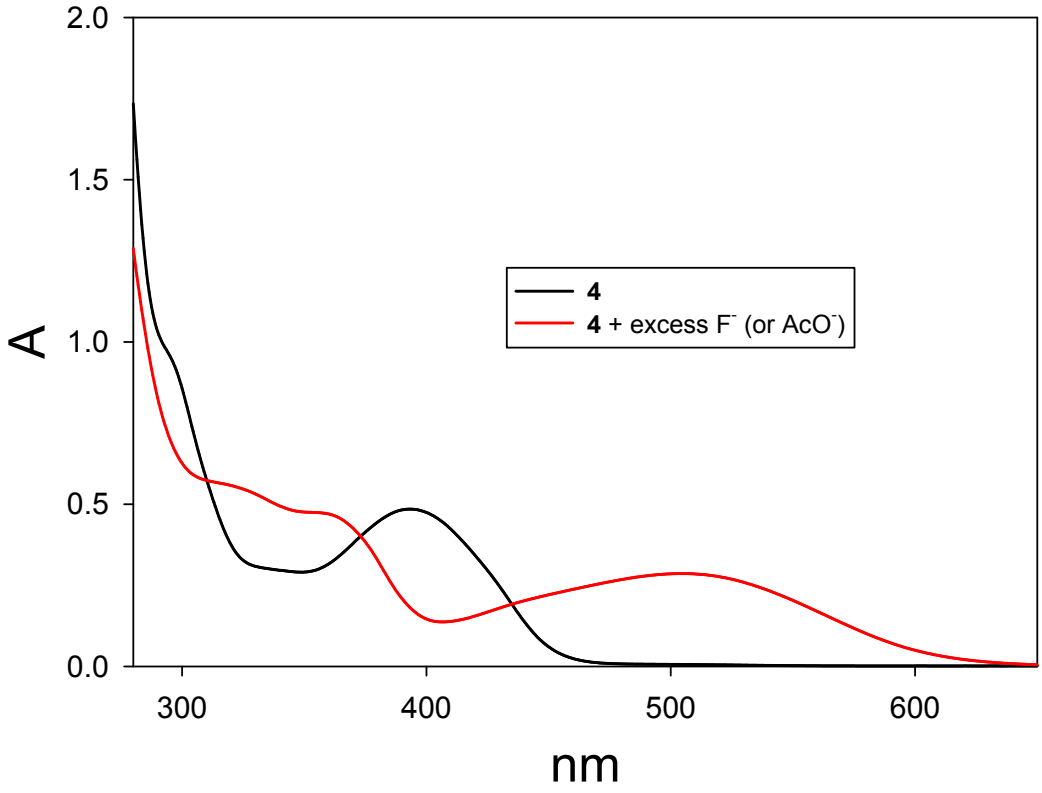

Figure S4. UV-vis absorption spectra of [**4**] before and after the addition of excess (TBA)F in DMSO at 25 °C.

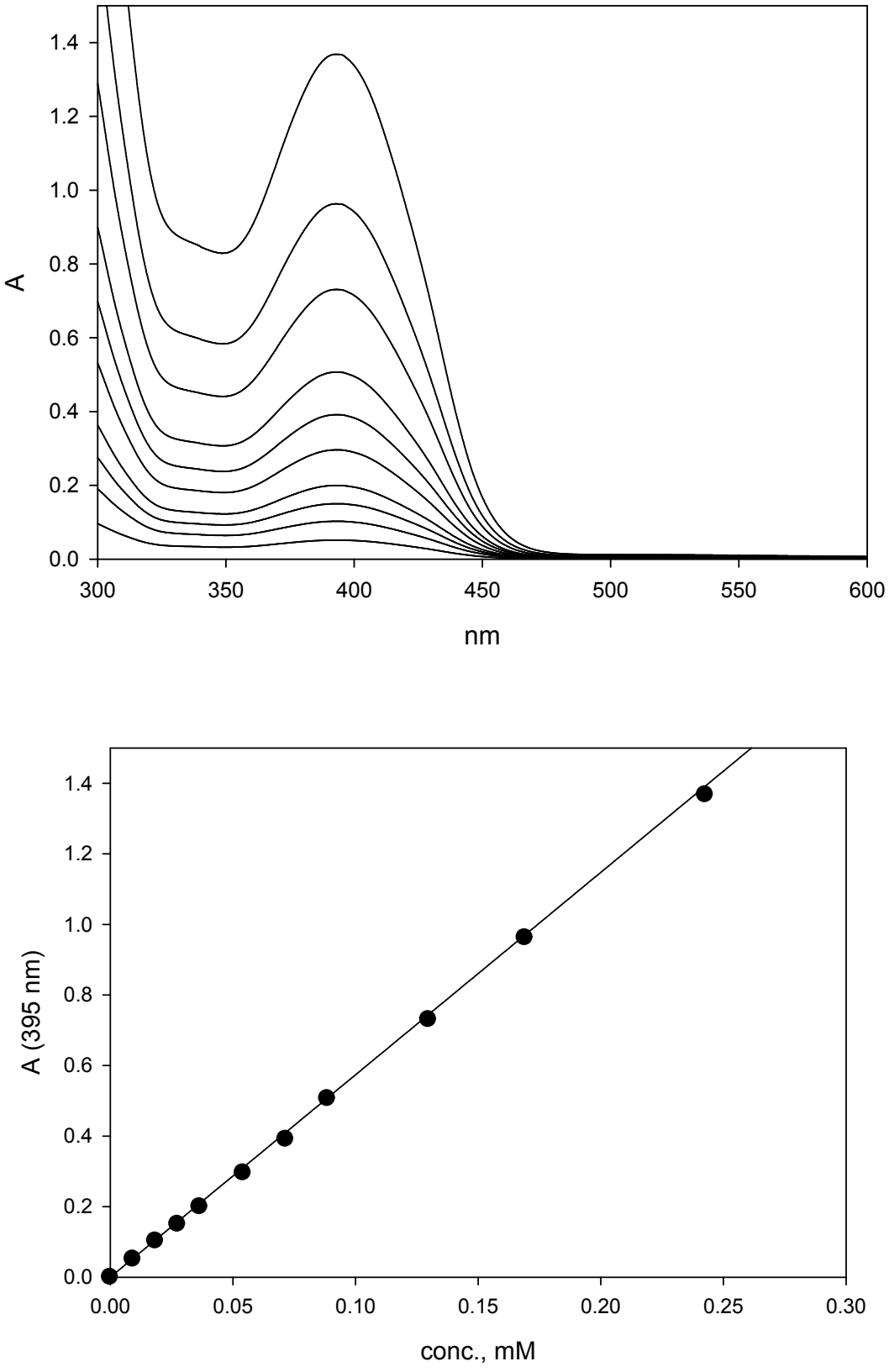

Figure S5. Adherence to the Lambert and Beer law for compound **4** in DMSO: 1) Absorption spectra of **4** at increasing concentrations and b) Abs (395 nm) vs. concentration plot for **4** in DMSO at 25°C.

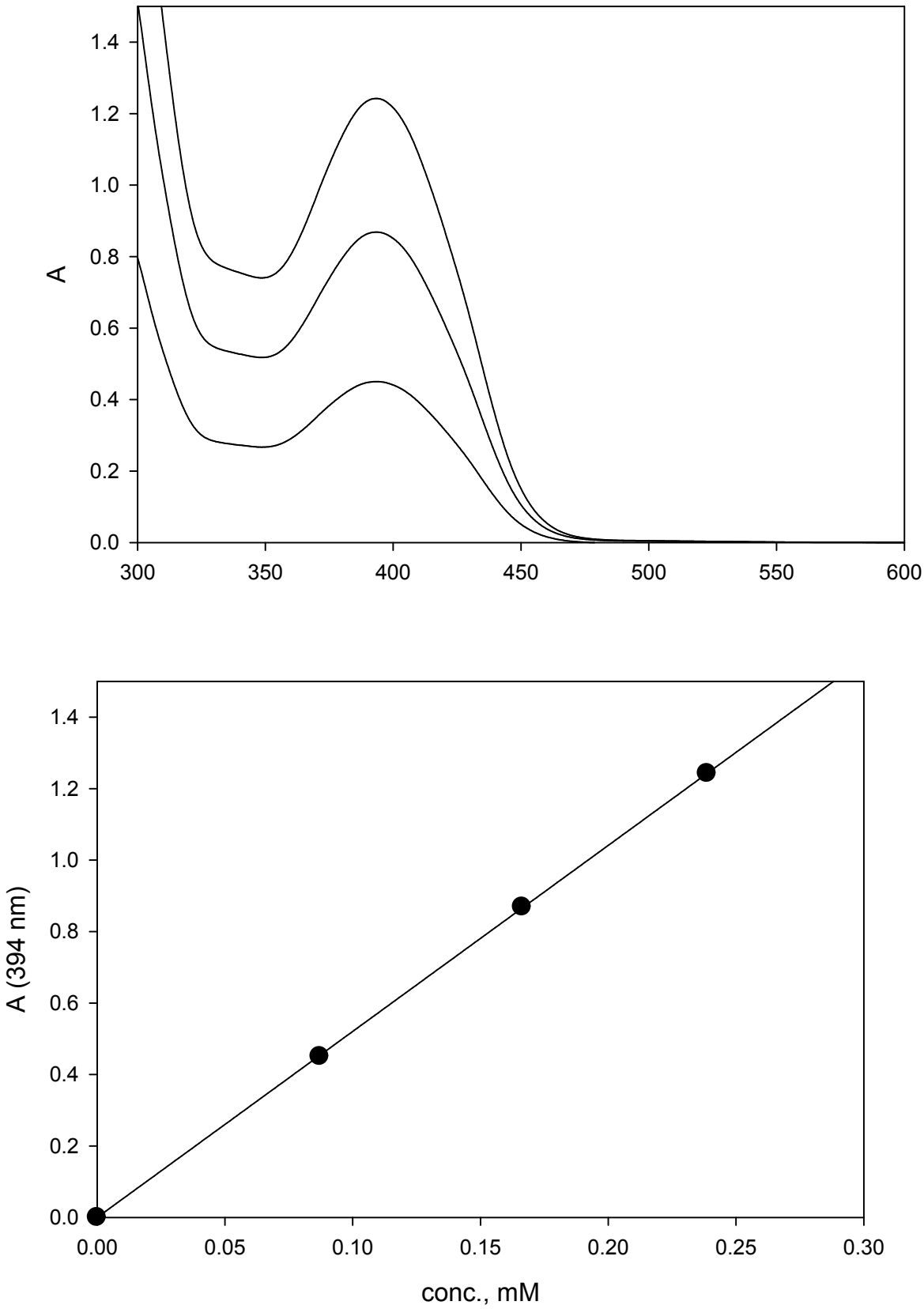

Figure S6. Adherence to the Lambert and Beer law for compound **5** in DMSO: 1) Absorption spectra of **5** at increasing concentrations and b) Abs (395 nm) vs. concentration plot for **5** in DMSO at 25°C (λ_{max} = 394 nm, ε = 5200 ± 30 M^{-1} cm^{-1}).

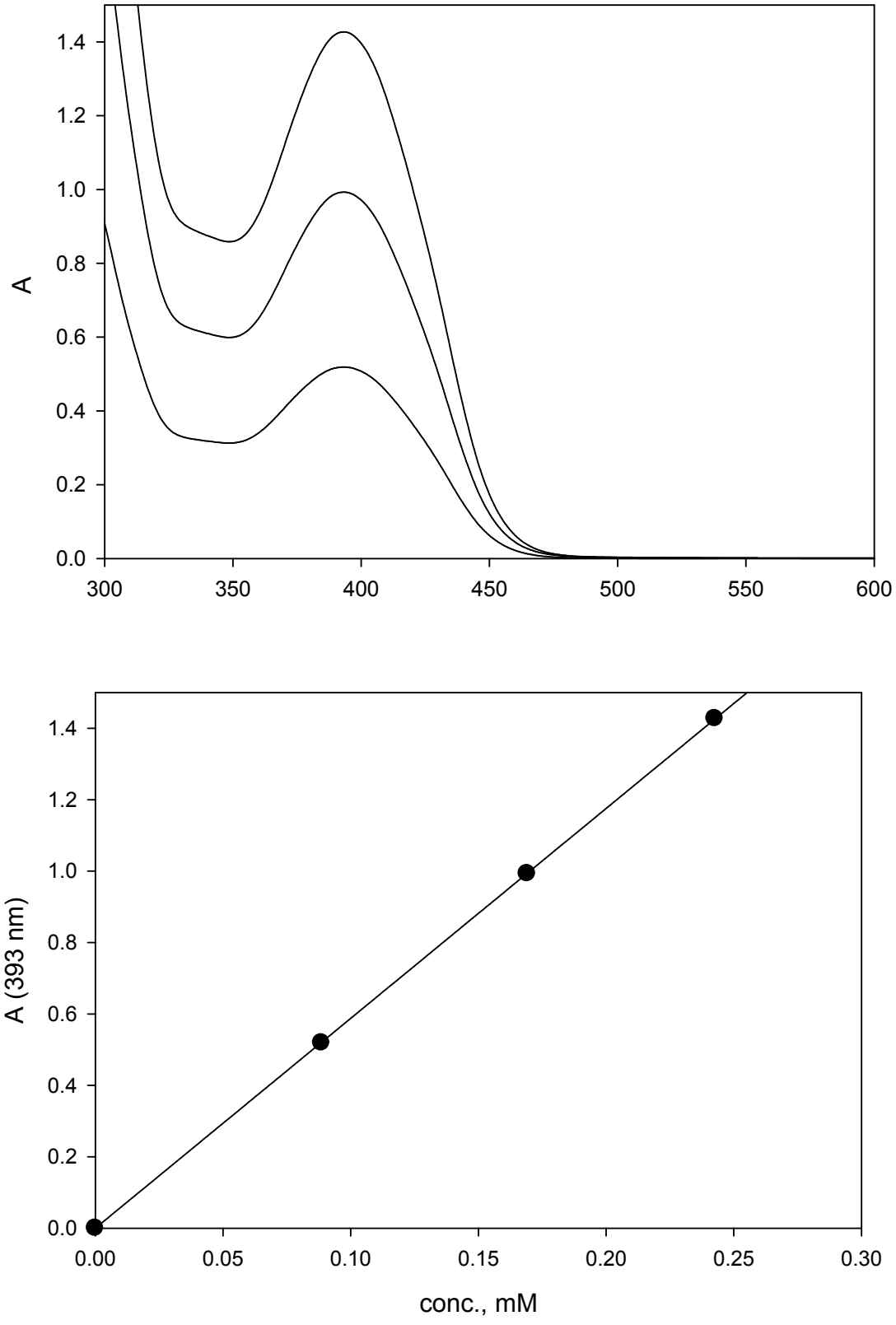

Figure S7. Adherence to the Lambert and Beer law for compound **6** in DMSO: 1) Absorption spectra of **6** at increasing concentrations and b) Abs (395 nm) vs. concentration plot for **6** in DMSO at 25°C. (λ_{max} = 393 nm, ε = 5880 ± 30 M^{-1} cm^{-1}).

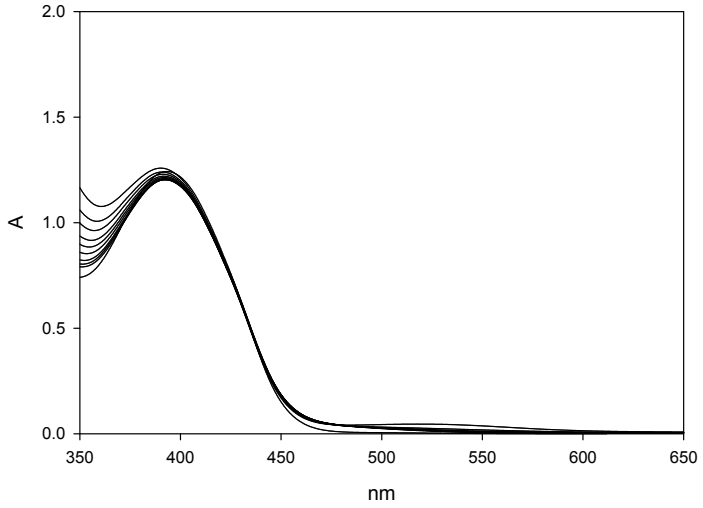

a)

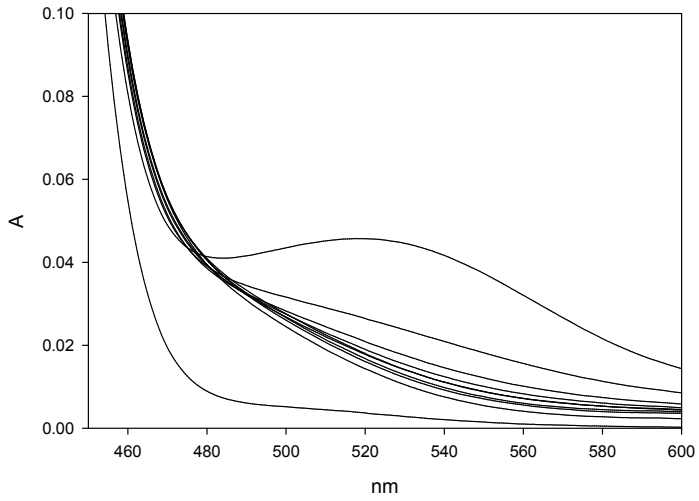

b)

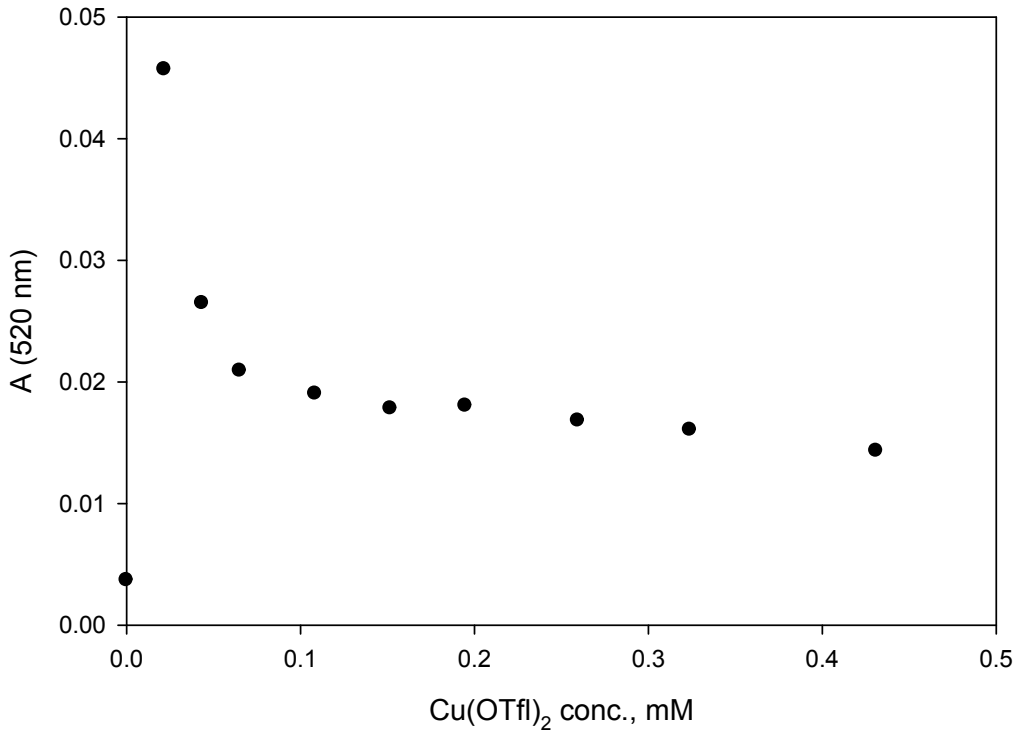

c)

Figure S8. a) Family of spectra obtained by addition of small aliquots of $Cu(OTf)_2$ to a 2.4 x 10^{-4}M solution of **5** in DMSO at 25°C; b) magnification of the region between 460 and 600 nm; c) Plot of Abs. vs. Cu(II) concentration at 520 nm.

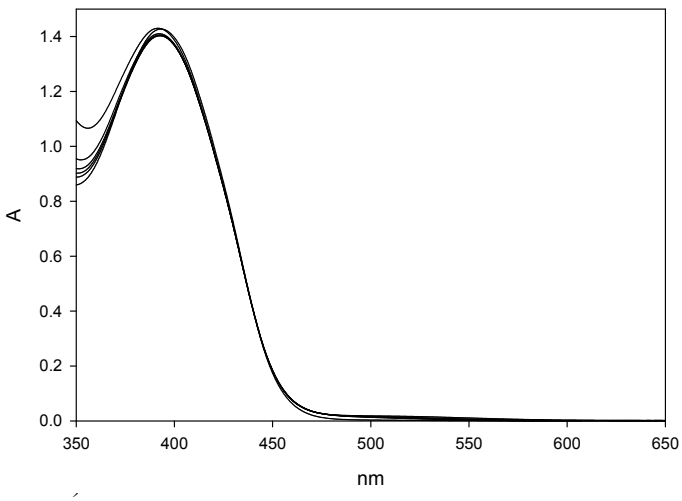

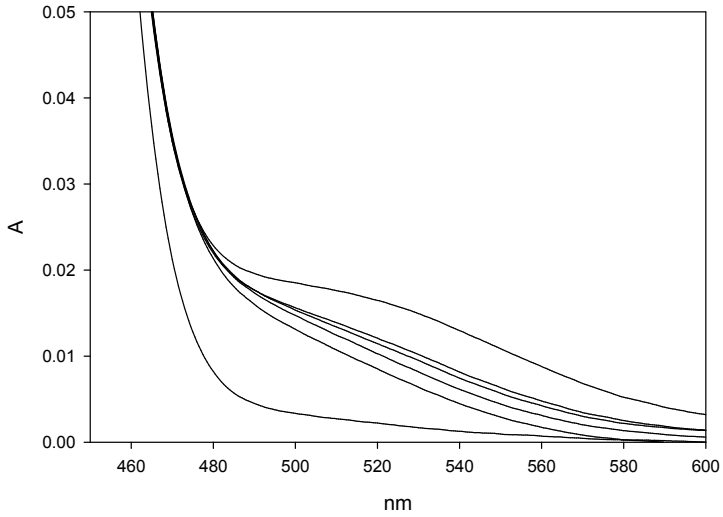

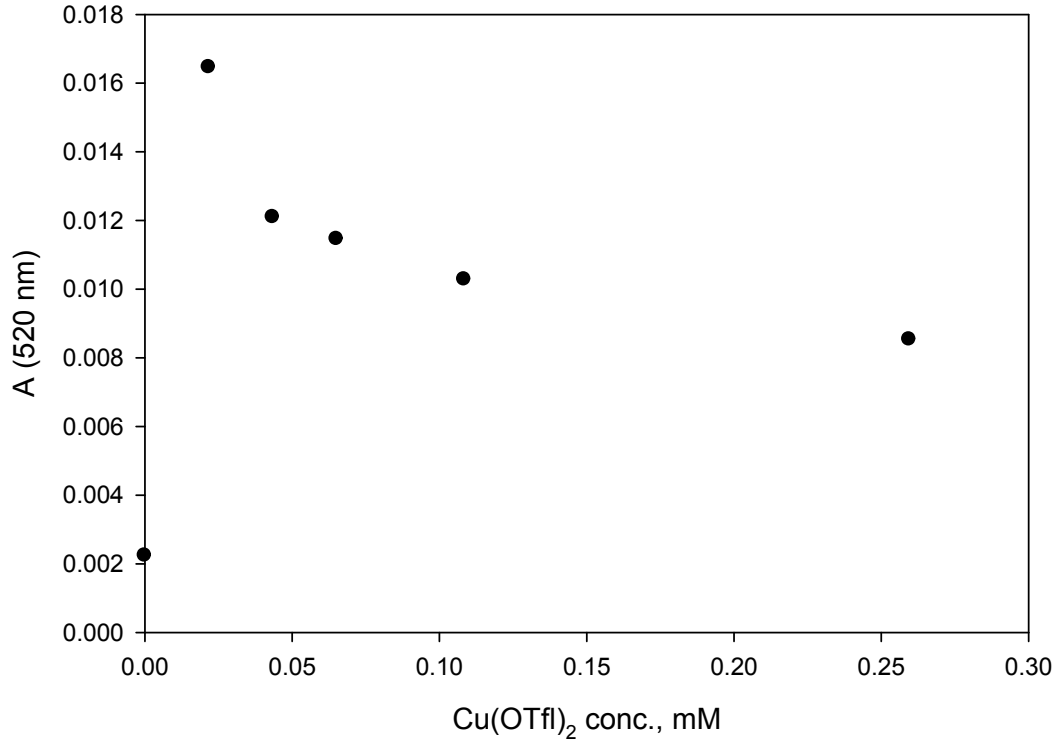

c)

Figure S9. a) Family of spectra obtained by addition of small aliquots of $Cu(OTf)_2$ to a 2.4 x 10^{-4}M solution of **6** in DMSO at 25°C; b) magnification of the region between 460 and 600 nm; c) Plot of Abs. vs. Cu(II) concentration at 520 nm.

Another set of experiments was executed by adding increasing aliquots of ligand **4** to a solution of $Cu(OTf)_2$ in DMSO (in the range 0.1 - 0.8 mM). Again, spectral variations in the 450 – 550 nm range were detected and a plot Abs (450 nm) vs. ligand **4** concentration is shown in Figure S10 (the data were taken at 450 nm in order to have a reliable comparison with the absorption of ligand 1 whose ε at λ > 480 nm cannot be confidently established due to low absorption).

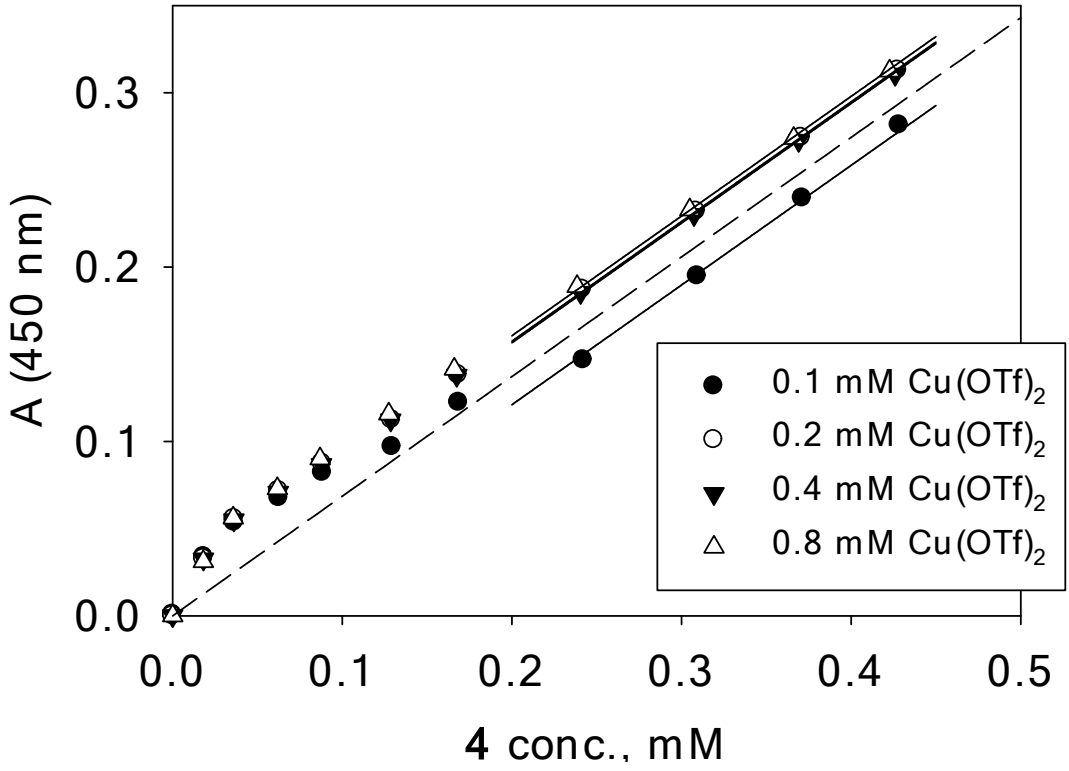

Figure S10. Plot of the absorbance changes at 450 nm of a solution of $Cu(OTf)_2$ x mM (x = 0.1, 0.2, 0.4 and 0.8) upon addition of **4** in DMSO at 25°C.

Two regions of the plot are readily identifiable, the first at low ([**4**] < 0.15 mM) the other at high ([**4**] > 0.2 mM) ligand concentration. In the latter region, the increase in the Absorbance is linear and the slope coincides with that of **4** (ε_{450} = 680). However, being the formation of a 1:1 complex with ligand **4** and Cu(II) which involves the coordination to the pyridyl ring ineffective in terms of spectral variation in that region, and considering the fact that the linear tract develops after reaching ca. 0.2 mM of **4** regardless of the initial Cu(II) concentration, we can assume that, at high ligand concentration ([**4**] > 0.2 mM), a 1:1 **4**-Cu(II) complex forms. As far as the first part of the plot is concerned, that at [**4**] < 0.1 mM, data could suggest the formation of a labile 2:1 Cu(II):**4** complex, in equilibrium with a 1:1 complex which becomes predominant at increasing ligand concentration. In the case of ligands **5** and **6**, the initial increase of the absorption in the 450 - 550 nm region is not observed (see Figures S11 and S12) as expected due to the difference in their coordination ability.

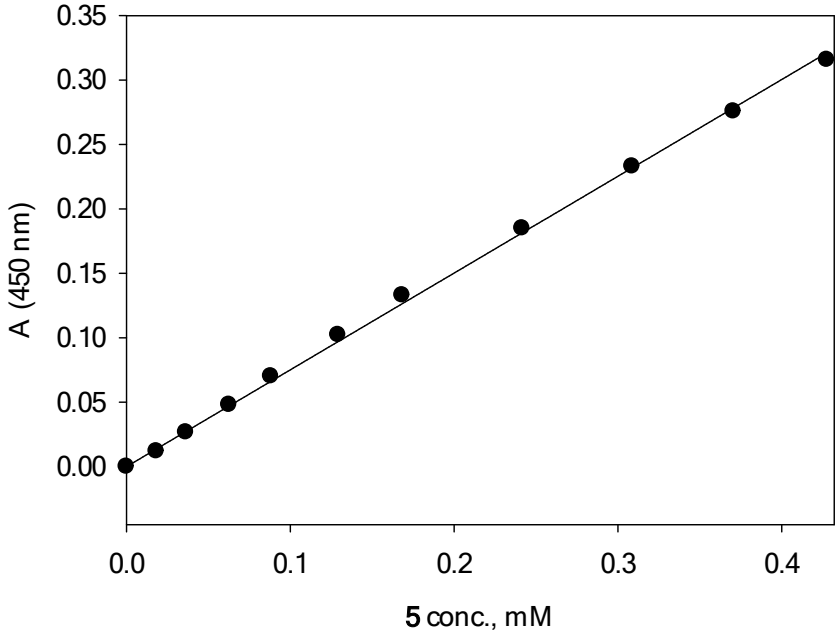

Figure S11. Plot of the absorbance changes at 450 nm of a solution of $Cu(OTfl)_2$ 0.2 mM upon addition of **5** in DMSO at 25°C.

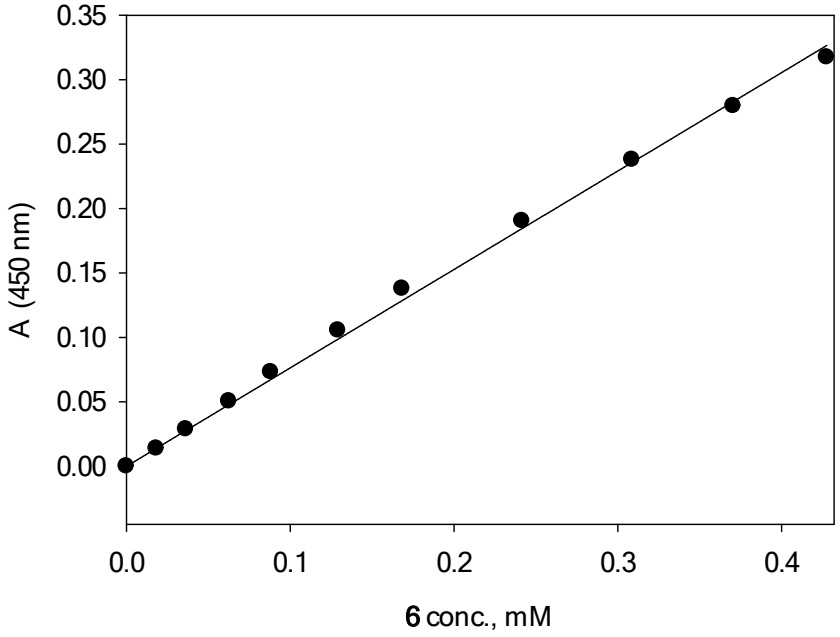

Figure S12. Plot of the absorbance changes at 450 nm of a solution of $Cu(OTf)_2$ 0.2 mM upon addition of **6** in DMSO at 25°C.

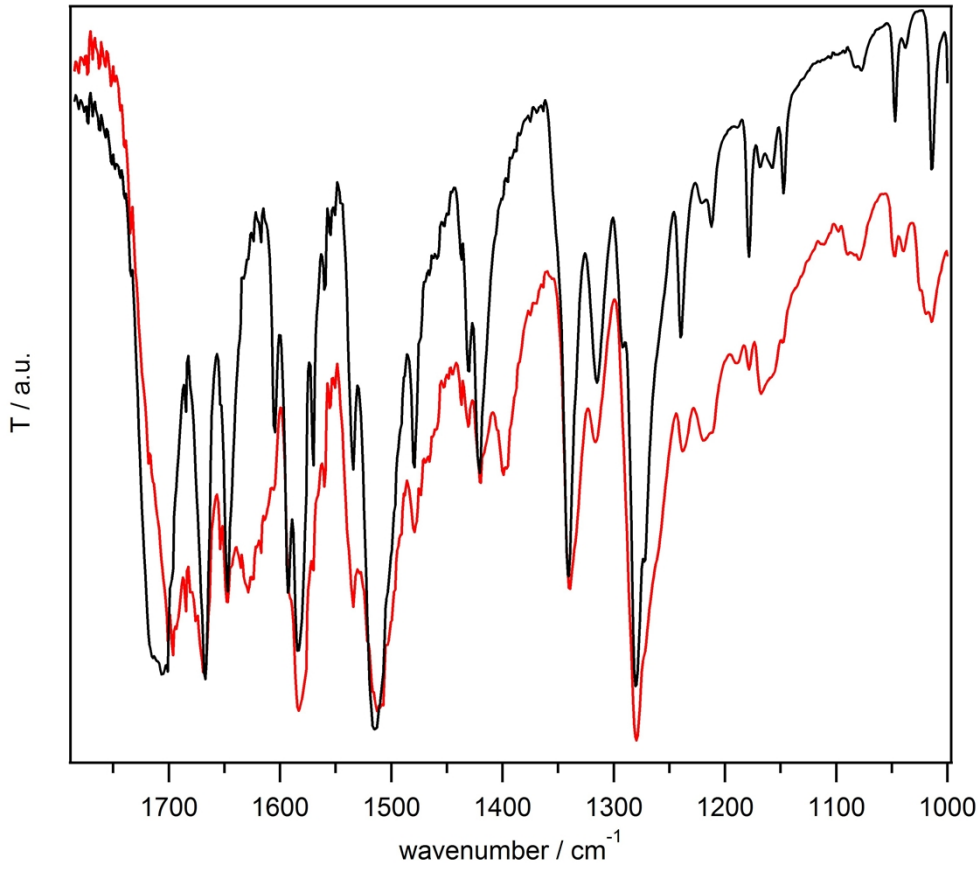

Figure S13. FT-IR spectra of ligand **4** in solid state (black) and the xerogel (red).

Details on the X-Ray Crystallographic Analysis

Experimental

Single crystal of [(**2**)$_2$CuCl$_2$](R=isobutyl) suitable for X-ray single crystal analysis was obtained at room temperature by partial evaporation from methanol solution. The intensities were collected on an Oxford Diffraction Xcalibur2 diffractometer with a Sapphire 3 CCD detector using graphite-monochromated MoKα radiation (λ = 0.71073 Å) at 295 K. *CrysAlisPro*[S2] program was used for the data collection and processing. The intensities were corrected for absorption using the multi-scan absorption correction method.[S2] The structure was solved by direct methods with *SHELXS-97*[S3] and refined by full-matrix least-squares calculations based on F^2 using *SHELXL-2013*[S3] integrated in *WinGX*[S4] program package. Hydrogen atoms attached to nitrogen atoms were found in Fourier map and refined by using geometric restraint on N–H distances (DFIX 0.86). All other hydrogen atoms were treated using appropriate riding models, with *SHELXL-2013* defaults.[S3] Restraints on anisotropic displacement parameters were applied in the refinement of C15, C28, C29 and O2 atoms. ADDSYM module in *PLATON* program,[S5] as well as CheckCIF report on the consistency and integrity of crystal structure determination (C level Alert) detected (pseudo) centre of symmetry. Refinement of this structure in suggested space group *C*2/*c* resulted in significantly higher *R* value and caused severe refinement problems of leucine moiety atoms. Details of crystal data, data collection, and refinement parameters are given in Table S2. *PLATON*[S5] and *Mercury*[S6] programs were used for structure analysis and molecular and crystal structure drawings preparation. The CCDC 1037543 contains the supplementary crystallographic data for this paper. These data can be obtained free of charge from The Cambridge Crystallographic Data Centre via www.ccdc.cam.ac.uk/data_request/cif.

Table S2. X-ray crystallographic data for [(**2**)$_2$CuCl$_2$](R=isobutyl)

Formula	$C_{30}H_{42}Cl_2CuN_6O_8$
Formula weight	749.13
Crystal system	monoclinic
Space group	*C* 2 (No. 5)
Unit cell dimensions	
a / Å	16.8441(7)
b / Å	7.0162(3)
c / Å	31.0687(11)
β / °	95.858(4)
V / Å^3	3652.6(3)
Z	4
$D_{calc.}$ / g cm^{-3}	1.362
Absorption coef. μ / mm^{-1}	0.798
θ range / °	4.292 – 27.494
Collected reflections No.	16896
Independent reflections. No. / $R_{Int.}$	8345 / 0.0319
Reflections No. $I \geq 2\sigma(I)$	6302
Data / Restraints / Parameters	8345 / 29 / 442
Flack parameter, *x*	-0.007(16)
Goodness-of-fit on F^2, *S*	1.009
R [$I \geq 2\sigma(I)$] / *R* [all data]	0.0417 / 0.0672
wR [$I \geq 2\sigma(I)$] / *wR* [all data]	0.0840 / 0.0927
Max. / min. el. dens. / e Å^{-3}	0.236 / -0.311

Structure description

The four coordinating atoms in the basal plane N1, N4, Cl1 and Cl2 are nearly coplanar. The largest deviation from the mean plane is 0.031(1) Å for the Cl2 atom, and the metal center is displaced only 0.019(1) Å from the mean plane.

Two pyridyl rings bonded to Cu atom are almost parallel, the dihedral angle being 4.3(2)^{o} (Fig. S14). Intrachain pyridyl rings are aproximately coplanar, while those between the chains are mutually parallel. The conformation of two **2** (R=isobutyl) molecules bonded to the Cu atom differs, especially in the leucine moiety as shown by values of equivalent torsion angles given in Table S3.

Table S3 Selected bond distances (Å), angles and torsion angles (^{o}) for [(**2**)$_2$CuCl$_2$](R=isobutyl)

Cu1−N1	2.005(3)	Cu1−N4	2.005(3)
Cu1−Cl1	2.2699(14)	Cu1−Cl2	2.2757(13)
Cu1−O1	2.755(3)		
N1−Cu1−N4	177.10(18)	N4−Cu1−Cl1	90.88(11)
N1−Cu1−Cl1	89.96(11)	N4−Cu1−Cl2	88.91(10)
N1−Cu1−Cl2	90.28(11)	Cl1−Cu1−Cl2	179.36(6)
N1−Cu1−O1	95.54(13)	Cl1−Cu1−O1	87.84(8)
N4−Cu1−O1	87.29(12)	Cl2−Cu1−O1	91.56(8)
C8−N3−C9−C10	-96.4(5)	C23−N6−C24−C25	69.4(7)
C8−N3−C9−C12	140.6(4)	C23−N6−C24−C27	-61.0(6)
C12−C9−C10−O3	111.1(5)	C27−C24−C25−O7	151.6(6)

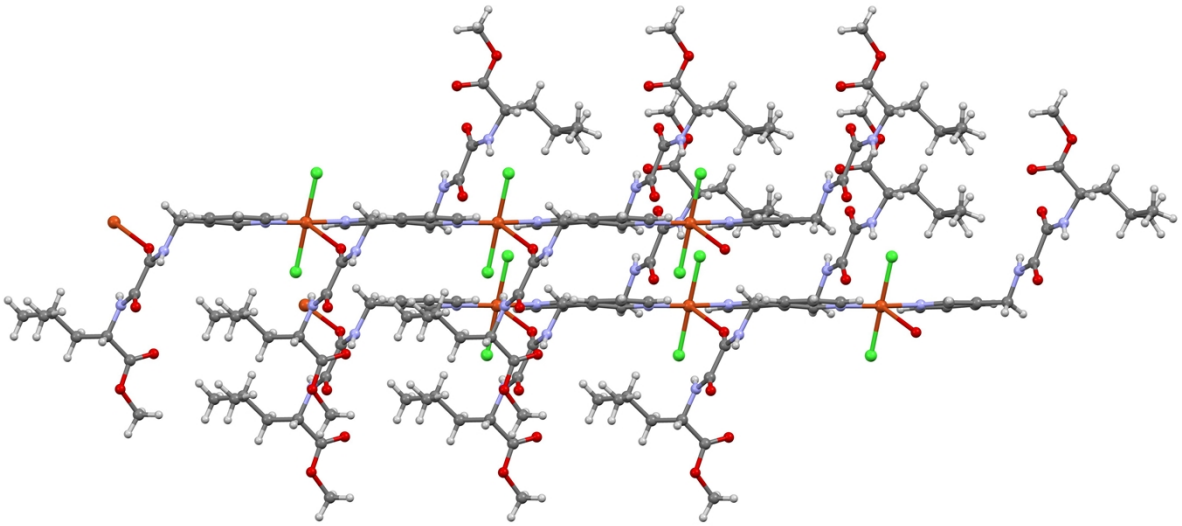

Fig. S14 Part of the crystal structure of complex [(**2**)$_2$CuCl$_2$](R=isobutyl), showing two one-dimensional coordination chains and disposition of pyridine rings.

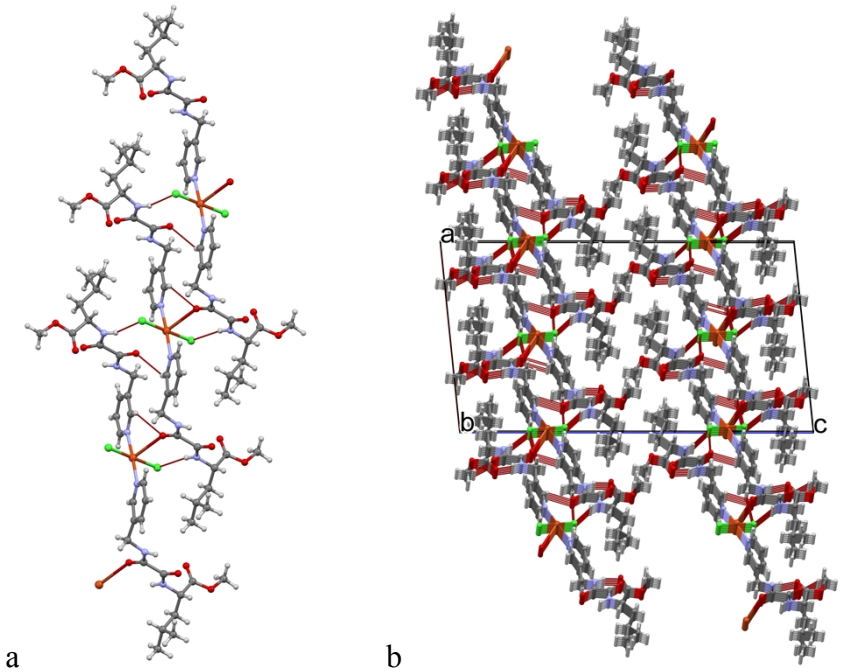

Fig. S15 a) Part of the crystal structure of complex [(**2**)$_2$CuCl$_2$](R=isobutyl), showing N–H···Cl and C–H···O intermolecular hydrogen bonds in one-dimensional coordination chain. b) Crystal packing diagram of complex [(**2**)$_2$CuCl$_2$](R=isobutyl), showing two-dimensional sheets formed by N–H···O, C–H···Cl and C–H···O hydrogen bonds as well as one C–H···π interaction.

Table S4 Intermolecular hydrogen-bonding geometry for [(**2**)$_2$CuCl$_2$](R=isobutyl)

D–H···A	D–H (Å)	H···A (Å)	D···A (Å)	D–H···A	Symmetry codes
N3–H3N···Cl1	0.86(3)	2.52(3)	3.363(4)	168(3)	–1/2+x, –1/2+y, z
N6–H6N···Cl2	0.86(3)	2.42(4)	3.226(4)	157(3)	1/2+x, 1/2+y, z
C5–H5···O5	0.93	2.47	3.085(5)	124	–1/2+x, –1/2+y, z
C20–H20···O1	0.93	2.50	3.129(5)	125	1/2+x, 1/2+y, z
N2–H2N···O3	0.86(3)	2.32(4)	3.124(6)	157(3)	x, 1+y, z
N5–H5N···O7	0.86(3)	2.49(4)	3.228(6)	145(4)	x, –1+y, z
C1–H1···Cl1	0.93	2.85	3.509(5)	128	x, 1+y, z
C6–H6A···Cl1	0.97	2.76	3.626(4)	149	–1/2+x, 1/2+y, z
C11–H11A···O2	0.96	2.36	3.269(7)	158	x, –1+y, z
C21–H21B···Cl2	0.97	2.81	3.703(5)	153	1/2+x, –1/2+y, z
C6–H6A···*Cg*1[a]		2.98	3.509(5)	116	–1/2+x, 1/2+y, z

[a] *Cg*1 is the centroid of N4/C16-C20 pyridine ring.

References

S1 Z. Džolić, M. Cametti, A. Dalla Cort, L. Mandolini and M. Žinić, *Chem. Commun.*, 2007, 3535.

S2 Oxford Diffraction, Xcalibur CCD System. *CrysAlisPro*; Agilent Technologies, Abingdon, England, 2013.

S3 G. M. Sheldrick, *Acta Crystallogr.*, 2008, **A64**, 112.

S4 L. J. Farrugia, *J. Appl. Crystallogr.*, 2012, **45**, 849.

S5 A. L. Spek, *Acta Crystallogr.*, 2009, **D65**, 148.

S6 F. Macrae, P. R. Edgington, P. McCabe, E. Pidcock, G. P. Shields, R. Taylor, M. Towler and J. van de Streek, *J. Appl. Crystallogr.* 2006, **39**, 453.